Computer problems

accompanying Lecture Notes on:

Atmospheres and Oceans on Computers: Fundamentals

Lars Petter Røed
Norwegian Meteorological Institute
P. O. Box 43 Blindern
0313 Oslo, Norway

and

Department of Geosciences
University of Oslo
Section Meteorology and Oceanography
P. O. Box 1022 Blindern
0315 Oslo, Norway

Fall 2016

Printed
November 28, 2016

PREFACE

Solving problems in Meteorology and Oceanography on computers using numerical methods consist of five phases:

1. Develop a numerical analogue of the continuous mathematical problem
2. Write, compile and run a computer code (usually written in Fortran 90/95 or 2003) on a given computer based on the numerical analogue constructed during Phase 1 and file the results
3. Visualize the results derived in Phase 2
4. Verify that the results you get are what you instructed the computer to provide
5. Perform an evaluation of the results to satisfy yourself and others that the numerical solution make sense in terms of the inherent physics of the problem

Phases 3, 4, and 5 are part of what is referred to as Quality Assurance procedures (*GESAMP*, 1991; *Lynch and Davies*, 1995; *Røed*, 2014). These procedures have four steps:

1. *Debugging* - to check that the code has no formal errors, and that the code is a true replica of the numerical analogue
2. *Calibration* - to specify appropriate numbers for parameters and coefficients appearing in the parameterizations, also referred to as tuning
3. *Verification* - to check the results against whatever is known about the true solution. This may be an analytic solutions, solutions to simplified equations, specified benchmark solutions, or your own feeling about what the results should look like
4. *Validation* - to check the results against observations, for instance whether the forecast had any skill

These exercises are a companion to the GEF4510 Lecture Notes "Atmospheres and Oceans on Computers: Fundamentals". Students following the class are required to submit at least four of these exercises for evaluation and approval. The mandatory problems replace the mid term exam. Moreover, the problems must be approved before the student is allowed to take the (oral) exam. The number of problems are continuously amended and changed to adjust to the GEF4510 Lectures. Although only four problems are required for students following the lectures in GEF4510, I strongly encourage to solve as many of the problems as possible in order to get the necessary hands-on experience and insight into the five phases of numerical modeling listed above. While the lectures in GEF4510 gives detailed insight into how to develop and construct finite difference analogues to the continuous mathematical formulation of the governing equations, that is, Phase 1, experience and training in the four remaining phases can only be achieved by getting your fingers dirty.

Finally, I would like to thank the many colleagues who has contributed to the development of these exercises over the years, and to the many students for pointing out misprints and other mistakes.

This version is for the fall 2016. Good luck!

Blindern, November 28, 2016
Lars Petter Røed (sign.)

Revision history (most recent on top):

All revisions made by the author.

- ☞ Sep 15, 2016: Updated the Preface chapter and the front page.
- ☞ Oct 25, 2016: Updated Problem set 6.
- ☞ Nov 04, 2016: Updated Problem set 11.

Contents

List of Figures

1 Problem set: Truncation error in a recursion formula with two terms

All student are strongly recommended to do this problem, but it is not mandatory. The rationale is that

1. it is simple enough to enable you to refresh your knowledge of Fortran and your Fortran skills without having to write lengthy codes, and
2. it demonstrates the dramatic consequences of the presence of insignificant truncation errors always present in numerical computations.

a.

Let

$$\pi = 4\arctan(1),\ Z_1 = \pi, \text{ and } S_1 = \pi. \tag{1}$$

Compute

$$Z_{j+1} = 3.1Z_j - 2.1Z_1 \text{ and } S_{j+1} = \left(\frac{9.}{5.}\right) S_j - \left(\frac{4.}{5.}\right) S_1 \tag{2}$$

for $j = 1(1)N$. Compute also the *relative* error, that is,

$$\epsilon_j = \frac{Z_{j+1} - Z_j}{Z_j}, \tag{3}$$

for each j. Write π, Z_j, S_j and the relative error ϵ_j in percent. The output should be readable and self explanatory, e.g., should have headings for each column. Do the problem on different platforms (from handhelds to portables, PCs and supercomputers) available to you. Experiment by using 1) different constants in the recursion formulas, 2) double and single precision, and 3) different numbers of iterations (use at least $N = 1000$). Does it impact the results?

b.

Show analytically why the recursion formulas for Z_j and S_j actually should diverge from π. If one or both of the recursion recursion formulas does not diverge numerically explain why.

2 Problem set: Vertical Diffusive Mixing

In the ocean and atmosphere the vertical (and horizontal) heat exchange is dominantly a turbulent process, commonly commonly parameterized as a diffusion process. Hence the governing equation in its simplest form is

$$\partial_t \psi + \partial_z F = 0, \tag{4}$$

where $\psi = \psi(z,t)$ is the potential temperature, z is the vertical coordinate, t is time and F is the vertical component of the diffusive flux vector.

In its simplest form F is parameterized as a down-the-gradient diffusion, that is, as

$$F = -\kappa \partial_z \psi, \tag{5}$$

where κ is the diffusion coefficient[1]. From (4) we then get

$$\partial_t \psi = \partial_z \left(\kappa \partial_z \psi \right). \tag{6}$$

Note that since the exchange is due to turbulent mixing κ becomes a function of space and time. In this exercise we assume that the diffusion coefficient κ is a constant. Under these circumstances (6) reduces to

$$\partial_t \psi = \kappa \partial_z^2 \psi. \tag{7}$$

We underscore that ψ can be any active tracer like temperature, humidity and salinity, or a passive tracer like CO_2.

We will solve (7) numerically for two applications. The first is associated with mixing in the atmosphere, while the second is associated with mixing in the ocean. The mixing or diffusion coefficient in the two spheres are dramatically different. Relatively speaking all oceanic motion is slow compared to the atmosphere. This is also true regarding mixing. In fact the mixing coefficient in the ocean is a factor 10^{-4} less than in the atmosphere (*Gill,* 1982).

We assume that the two spheres are contained between two fixed z-levels. At these levels (7) is replaced by relevant boundary conditions. Regarding the atmosphere we assume that the bottom level is located at $z = 0$, while the top level $z = H$ is at the top of the planetary mixed layer. For the ocean application the top level is the surface at $z = 0$, while the bottom level, $z = -D$, is at the base of the oceanic mixed layer. Thus the atmospheric planetary boundary layer is contained in $z \in < 0, H >$, while the oceanic mixed layer is contained within $z \in < -D, 0 >$. We will assume that height of the atmospheric boundary layer is $H = 270m$, and that the oceanic boundary layer is $D = 30m$ deep.

In both cases we will seek the numerical solution for time $t \in [0, N\Delta t]$ with $N = 1201$. Here Δt is the time step and N is the total number of time steps. Furthermore we let $H, D = (J_{max} - 1)\Delta z$ where Δz is the space increment[2] and $J_{max} = 27$ is the total number of grid points including the two boundary points at the bottom and top levels.

[1] In three dimensional space F becomes a vector and (4) becomes $\partial_t \psi + \nabla \cdot \mathbf{F} = 0$ in which case the diffusive flux vector is parameterized as $\mathbf{F} = -\boldsymbol{\mathcal{D}} \cdot \nabla \psi$, where $\boldsymbol{\mathcal{D}}$ is a tensor, that is, $\boldsymbol{\mathcal{D}} = \kappa_{mn} \mathbf{i}_m \mathbf{i}_n$ for $m = n = 1, 2, 3$.

[2] Also commonly referred to as the mesh or grid size.

a.

Develop a numerical scheme (or finite difference approximation) that is forward in time and centered in space for (7). Show that the derived scheme is stable under the condition $K \leq \frac{1}{2}$, where

$$K = \frac{\kappa \Delta t}{\Delta z^2}. \tag{8}$$

b.

Next develop a finite difference approximation for (7) that is centered in both time and space, and show that this algorithm is unconditionally unstable in a numerical sense.

c.

Let $K = 0.45$, $\kappa_A = 30$ m^{2}s^{-1}, and $\kappa_O = \kappa_A \cdot 10^{-4}$, respectively. Compute the time steps you will have to use for the atmospheric and oceanic applications, respectively. The time steps are vastly different. Discuss why this is so, and its possible consequences.

d.

Consider first an atmospheric application. We assume that initially the temperature distribution is sinusoidal in height as shown in the left-hand panel of Figure 1, that is,

$$\psi(z, 0) = \psi_0 \sin(\frac{\pi z}{D}), \quad z \in [0, H], \tag{9}$$

where $\psi_0 = 10^{\text{o}}$C. Furthermore we let the temperature at the bottom level (or surface) $z = 0$ and the top level $z = D$ be fixed at the freezing point for all times, that is,

$$\psi(0, t) = \psi(D, t) = 0^{\text{o}}\text{C} \quad \forall t. \tag{10}$$

Use the stable forward in time, centered in space scheme developed under item **a.** to find the numerical solution to (7) for two cases; one with $K = 0.45$ and a second with $K = 0.55$. Plot the results for $n = 0, 100, 200, 600,$ and 1200 in which the height and temperature are made dimensionless by dividing through by D and ψ_0, respectively.

Derive the analytic solution to (7) given the initial condition (9) and the boundary conditions (10). Assess and discuss the solutions by comparing the numerical and analytic solutions. Explain in particular why the solution for $K = 0.55$ develops a "saw tooth" pattern.

e.

Consider next an oceanographic application. In this case we assume that the initial condition is

$$\psi(z, 0) = 0^{\text{o}}\text{C}, \quad z \in [-D, 0], \tag{11}$$

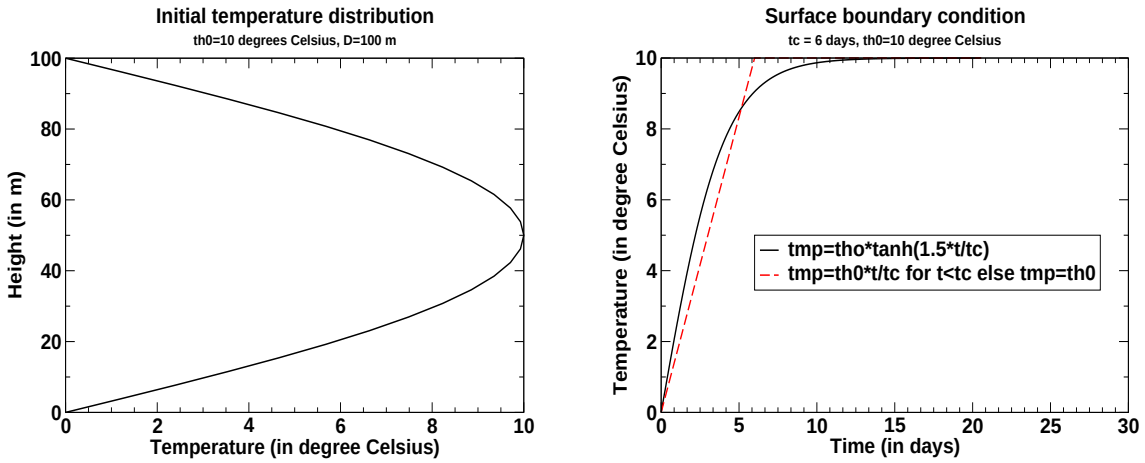

Figure 1: Left-hand panel displays the initial temperature distribution according to (9), while the right-hand panel shows the time evolution of the surface temperature according to (12) and (13), respectively.

throughout the water column. Thus the initial condition is the trivial solution to (7). In contrast to the atmospheric application the diffusion process is generated by letting the ocean surface be heated from above. Specifically, we let the boundary condition at $z = 0$ increase from zero to a fixed temperature $\theta_0 = 10^o$C after some finite time. This can be achieved either by letting the boundary condition be specified according to

$$\psi(0,t) = \psi_0 \begin{cases} \frac{t}{t_c} & ; \quad 0 < t < t_c \\ 1 & ; \quad t \geq t_c \end{cases} , \tag{12}$$

where $t_c = 6$ days determines how fast the surface temperature reaches its final temperature ψ_0 (cf. the right-hand panel of Figure 1), or by using a hyperbolic tangent (a good function), that is,

$$\psi(0,t) = \psi_0 \tanh(\frac{\gamma t}{t_c}) \tag{13}$$

where $\gamma = 1.5$ together with t_c determines how fast the temperature approaches its final temperature (cf. the right-hand panel of Figure 1). At the bottom of the ocean mixed layer $z = -D$ the temperature is fixed at the freezing point. Thus

$$\psi(-D,t) = 0^o\text{C} \tag{14}$$

Again choose the time step so that $K = 0.45$. Plot the results for $n = 0$, $n = 100$, $n = 200$ and $n = 400$. Use either (12) or (13) as your surface boundary condition.

Assess and discuss the solution. In particular you are asked to compare the solution with the steady state solution to (7), that is, the solution as $t \to \infty$ given the above initial and boundary conditions.

3 Problem set: Vertical Mixing in a coupled Atmosphere-Ocean

We will investigate the evolution of the temperature, say T, in a coupled atmosphere-ocean model in which the only active process is heat diffusion by vertical mixing, all other motion and processes being inhibited. Thus the the temperature is governed by the internal heat equation. In its simplest form, neglecting radiation and all other possible sources and sinks it becomes

$$\partial_t T + \partial_z F = 0, \tag{15}$$

where F is the vertical component of the diffusive heat flux due to turbulent mixing, and z is the vertical coordinate. As is common we parameterize the heat flux as Fickian diffusion, that is,

$$F = -\kappa \partial_z T, \tag{16}$$

where κ is the eddy diffusivity or mixing coefficient. Since the eddy diffusivity is a property of the motion rather than the fluid, it normally varies in time and space. Nevertheless, we will assume it to be constant. We note, however, that it is vastly different in the two spheres (*Gill*, 1982), the ocean being sluggish compared the atmosphere, in fact, $\kappa_O = 10^{-4}\kappa_A$ as given in Table 1, where κ_A is associated with the atmosphere and κ_O with the ocean.

Your task is to solve (15) for the time span $t \in \langle 0, T]$. In this we assume that the atmosphere and the ocean span the vertical space $z \in [-H, D]$, where D and H are considered to be constants, and $z \in < 0, D >$ spans the atmospheric boundary layer (ABL) and $z \in < -H, 0 >$ spans the oceanic mixed layer (OML) so that $z = 0$ is the location of the interface between them. Values for D and H are given in Table 1.

To avoid heat to accumulate at the interface between the two spheres we require that the oceanic heat flux toward's the interface is balanced by the atmospheric heat flux away from the interface. Any imbalance implies that ice is formed at the interface. Similarly we require that the temperature itself is continous at the interface. Thus

$$F_O = F_A \quad \text{and} \quad T_O = T_A \quad \text{at} \quad z = 0, \tag{17}$$

where subscript A, O refers to the atmosphere and ocean respectively. Furthermore we fix the temperatures at the bottom of the OML and top of the ABL to be respectively T_B and T_T, where T_B and T_T are given in Table 1. Thus we require

$$T_O = T_B \quad ; \quad z = -H, \tag{18}$$
$$T_A = T_T \quad ; \quad z = D. \tag{19}$$

Finally we let the temperature initially be constant and equal the temperature at the bottom of the OBL everywhere except at the top of the ABL where (18) prevails. Thus

$$T_A(z, 0) = T_O(z, 0) = T_B \quad ; \quad -H \leq z < D, \tag{20}$$
$$T_A(D, 0) = T_T \quad ; \quad z = D. \tag{21}$$

Symbol	Description	Value	Unit
κ_A	Atmospheric diffusion/mixing coefficient	30.0	m^2s^{-1}
κ_O	Oceanic diffusion/mixing coefficient	$3.0{\cdot}10^{-3}$	m^2s^{-1}
D	Height of ABL	270.0	m
H	Depth of OML	30.0	m
T_T	Temperature at the top of ABL	0.0	^{o}C
T_B	Temperature at the bottom of the OML	10.0	^{o}C

Table 1: Parameter values used in this Problem set

a.

Please explain why we need exactly the specified number of boundary and initial conditions in space and time as given by (17) -(21)?

b.

Show that the stationary solution to (15) satisfying the boundary conditions is

$$T = \begin{cases} -\gamma\kappa_A(z+H) + T_B & -H \le z < 0, \\ -\gamma\kappa_O(z-D) + T_T & 0 \le z \le D, \end{cases} \tag{22}$$

where

$$\gamma = \frac{T_B - T_T}{\kappa_A H + \kappa_O D}. \tag{23}$$

c.

Develop a numerical scheme, using finite difference approximations, that is forward in time and centered in space (an FTCS scheme) to replace the continuous equations (15) for the two spheres. Show that the derived scheme is stable under the conditions $K_A \le \frac{1}{2}$ and $K_O \le \frac{1}{2}$, where

$$K_A = \frac{\kappa_A \Delta t_A}{\Delta z_A^2} \quad \text{and} \quad K_O = \frac{\kappa_O \Delta t_O}{\Delta z_O^2}. \tag{24}$$

Here Δt_A and Δt_O are the time steps of the atmospheric and oceanic parts, respectively, while Δz_A and Δz_O are the respective space increments.

d.

Let $j_A = 1(1)J_A + 1$ denote the counter in the atmospheric part and $j_O = 1(1)J_O + 1$ the counter in the oceanic part, where $j_A = 1$ is associated with $z = 0$ and $j_O = 1$ is associated with

$z = -H$. Thus the interface is associated with $j_O = J_O + 1$. Show that under these circumstances $D = J_A \Delta z_A$ and $H = J_O \Delta z_O$, and hence that the ratio between the time steps is

$$\frac{\Delta t_A}{\Delta t_O} = \frac{\kappa_O K_A}{\kappa_A K_O} \left(\frac{\Delta z_A}{\Delta z_O} \right)^2 = \frac{\kappa_O K_A}{\kappa_A K_O} \left(\frac{D J_O}{H J_A} \right)^2 . \tag{25}$$

e.

Let us for a moment assume that there is an equal amount of grid points in the two spheres, that is, $J_A = J_O = J$, and that $K_A = K_O = K$. Use (25) and the numbers given in Table 1 to show that under these circumstances $\Delta t_A \ll \Delta t_O$, that is, the time step you have to use for the atmospheric part is much less than the for the oceanic part. Please discuss why there is such a difference in the time steps, and the possible consequences it has in terms of physics and numerics under the condition that $K = 0.45$.

f.

Next let us assume that $K_O = K_A = K = 0.45$, but that $J_A \neq J_O$. If we let $\Delta t_A = \Delta t_O$ then $\Delta z_O \neq \Delta z_A$, and if we let $\Delta z_O = \Delta z_A$ then $\Delta t_O \neq \Delta t_A$. From a numerical point of view it is advantageous to let $\Delta t_A = \Delta t_O$. Please explain why.

g.

Next let $\Delta t_A = \Delta t_O$ and $J_O = J_A = J$. Show that under these circumstances

$$\frac{K_O}{K_A} = \frac{\kappa_O D^2}{\kappa_A H^2} \tag{26}$$

Does K_O satisfy the sufficient condition for stability? Please discuss possible implications regarding the growth factor.

h.

Use the FTCS scheme you developed under item **a**. to find the numerical solution to (15) that satisfies the initial and boundary conditions. Solve for two cases; one stable case in which $K_A = K_O = 0.45$ and a second unstable case in which $K_A = K_O = 0.55$. For both cases let $\Delta t_A = \Delta t_O = \Delta t$, $J_A = 28$ and $J_O = 301$. The latter implies that $\Delta z_O = 0.1$m. For the stable case please plot the vertical distribution of the potential temperature at the time levels $n = 0$ (the initial distribution), $n = 50$, $n = 500$, $n = 5000$, $n = 50000$ and $n = 500000$. For the unstable case please plot the distribution for the time levels $n = 0$, $n = 10$, $n = 20$, $n = 30$, $n = 40$ and $n = 50$. Compute the time in hours for each case and include a legend (cf. Figure 2).

Please keep the scale along the axes in the two cases so that the temperature range is $T \in [T_B, T_T]$ and the depth/height range is $z \in [-H, D]$. Preferably the plot should show the height/depth along the vertical axis and the temperature along the horizontal axis as shown in Figure 2, which conveniently shows the results for the stable case.

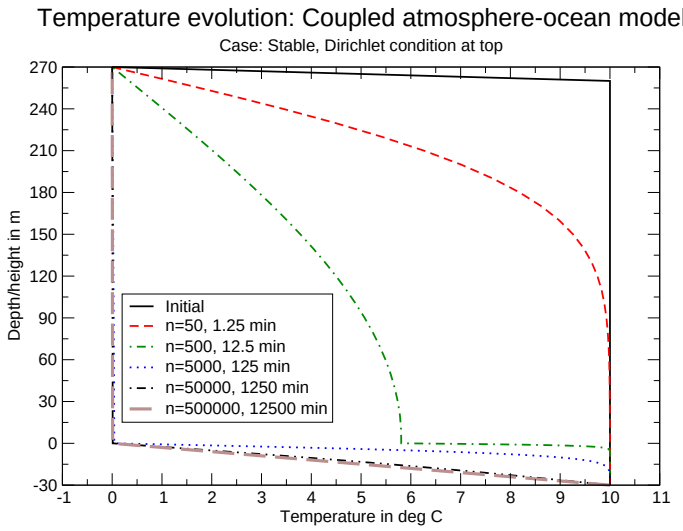

Figure 2: Depicted is the initial temperature distribution according to (20) and the time evolution of the vertical temperature profile for five time levels as time progresses.

i.

Assess and discuss the solution. In particular you are asked to compare the solution with the steady state solution (22), that is, the solution as $t \to \infty$ given the above initial and boundary conditions. Explain in particular why the solution for $K_A = 0.55$ develops a "saw tooth" pattern.

i.

What happens if the upper boundary condition is changed to a no flux condition, that is,

$$F_A|_{z=D} = -\kappa_A \partial_z \theta|_{z=D} = 0, \tag{27}$$

or $\partial_z \theta = 0$ at $z = D$? Solve for this case and plot the vertical potential temperature distribution in this case. Asses the the solution by comparing it to the former solution with a fixed temperature condition at the top of the ABL.

4 Problem set: Yoshida's equatorial jet current

Like *Yoshida* (1959) we consider an "infinite" equatorial ocean consisting of two immiscible layers with a density difference $\Delta\rho$ (Figure 3). The density of the lower layer equals the reference density ρ_0. The lower layer is thick with respect to the upper layer. At time $t = 0$ the ocean is at rest, at which time the thickness of the upper layer equals its equilibrium depth H. At this particular time the ocean is forced into motion by turning on a westerly wind (wind from the west).

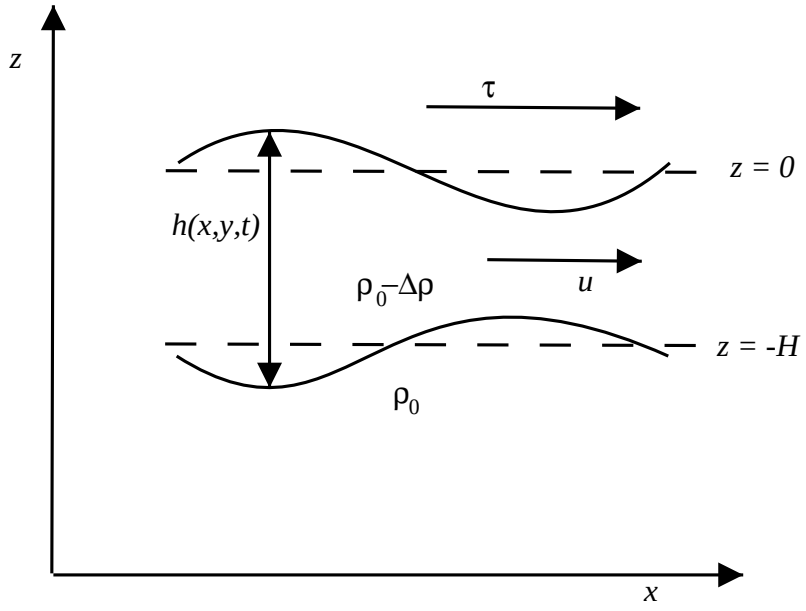

Figure 3: Sketch of a reduced gravity ocean model consisting of two layers with a density difference given by $\Delta\rho$.

The governing equations of such a "reduced gravity" model of the ocean, is

$$\partial_t u - \beta y v = \frac{\tau^x}{\rho_0 H} \tag{28}$$

$$\partial_t v + \beta y u = -g' \partial_y h \tag{29}$$

$$\partial_t h + H \partial_y v = 0 \tag{30}$$

Here $u = u(y,t)$ and $v = v(y,t)$ are the respectively the east-west and north-south components of the velocity in a Cartesian coordinate system (x, y, z) with x directed eastward along the equator, y directed northwards with $y = 0$ at the equator, and z directed along the negative gravitational direction as displayed in Figure 3. The impact of the Earth's rotation is given by the Coriolis parameter $f = 2\Omega \sin\phi$ where Ω is the Earth's rotation rate and ϕ is the latitude. The westerly wind is given by the wind stress component τ^x which is fixed in time. Furthermore,

we define the reduced gravity by $g' \equiv g(\Delta\rho_0/\rho)$ where g is the gravitational acceleration. The instantanuous thickness of the upper layer is given by $h = h(y,t)$.

Note that at the equator $f = 0$ and that it increases with increasing latitude. A simplified parameterization of this effect is through the so called β-plane approximation,

$$f = \beta y, \quad \text{hvor} \quad \beta = \partial_y f|_{y=0}. \tag{31}$$

We note the β is just a measure of the first term in a Taylor series of f at the equator. Thus it represents the first order effect effect of the impact of the change in the Earth's rotation rate with latitude.

Part 1:

a.

Show that the inertial oscillation[3] is eliminated by neglecting $\partial_t v$ in (29).

b.

Show that the system of equations (28) - (30) reduces to the ordinary differential equation

$$L^4\partial_y^2 v - y^2 v = aLy \tag{32}$$

where

$$L = \sqrt{\frac{c}{\beta}}, \quad a = \frac{\tau^x}{\rho_0 \beta L H}, \quad c = \sqrt{g'H} \tag{33}$$

under the condition that the inertial oscillation is eliminated.

c.

Explain why we are allowed to specify two boundary conditions. In the following we will assume that they are $v|_{y=0} = 0$ and $v|_{y\to\infty} = 0$.

d.

We make (32) dimensionless by letting $y = L\hat{y}$, $(u,v) = a(\hat{u},\hat{v})$, and $t = (\beta L)^{-1}\hat{t}$. Use the a direct elliptic solver, e.g., Gauss elimination, to solve the dimensionless expression of (32). Let $\Delta y = 0.1$ and plot $\hat{v}$ and $\hat{u}$ at time $\hat{t} = 1$ as a function of $\hat{y}$ from $\hat{y} = 0$ to $\hat{y} = 8$. We note that $v|_{y\to\infty} = 0$ and hence that $\hat{v}$ is different from zero at $\hat{y} = 8$. Explain how make use of the condition that $v|_{y\to\infty} = 0$.

[3] An oscillation in which the frequency equals the inertial frequency f.

e.

Discuss the numerical solution. Let $\tau^x = 0.1Pa$, $\beta = 2. \cdot 10^{-11}(ms)^{-1}$, $L = 275$km, $\rho = 10^3 kgm^{-3}$ and $H = 200m$. What is the maximum current in the equatorial jet for $\hat{t} = 1$?

f.

Solve (32) analytically. Hint: Make a series using Hermitian polynomials (se for instance *Abramowitz and Stegun*, 1965).

5 Problem set: Advection in the Atmosphere and Ocean

Since tracers such as temperature, salinity and humidity has a decisive impact on the dynamics of the atmosphere and ocean through its influence on the pressure distribution through density, advection (transport) of these tracers is of zero order importance to get correct.

Moreover, transport of contaminants in the ocean and atmosphere is one crucial element when discussing environmental issues. For instance emissions of radionuclide in one location are transported via atmospheric and oceanic circulation patterns to quite other locations. Other examples are transboundary advection of chemical substances such as sulfur (mostly atmosphere) and nutrients (mostly ocean). In the ocean advection processes are also of crucial importance regarding search and rescue, oil drift, and drifting objects (e.g, fish larvae, rafts, man overboard, ship wrecks, etc.)

Commonly all transport and spreading of the above are governed by an advection-diffusion equation, say

$$\partial_t \psi + \nabla \cdot (\mathbf{v}\psi) = \nabla \cdot (\kappa \nabla \psi) \tag{34}$$

where ψ is the concentration of the tracer, $\mathbf{v}$ is the three-dimensional wind or current vector and κ is the mixing or diffusion coefficient. We note that commonly the transport is associated with the advection part of (34), while the spreading is associated with the mixing part of (34). While the mixing was exemplified in Computer Problem #s 2 and 3 we focus on the advection part here. Thus we will neglect the mixing part in the remainder of this problem except in the very last question.

To make the problem as simple as possible, but no simpler, we reduce the advection problem to one dimension in space. Furthermore we let the advection speed be constant, say $\mathbf{v} = A\mathbf{i}$, where A is a constant. Thus we will consider numerical solutions to the equation

$$\partial_t \psi + u_0 \partial_x \psi = 0 \tag{35}$$

with appropriate boundary and initial conditions. To this end we will make use of three schemes, namely the *leapfrog scheme*, the *upwind* or *upstream* scheme and the *Lax-Wendroff* scheme.

Part 1: Analysis

a.

Show that the three schemes are numerically stable under the CFL condition

$$C = |u_0| \frac{\Delta t}{\Delta x} \leq 1 \tag{36}$$

where C is the Courant number, Δx is the space increment and Δt is the time step.

b.

Show that a forward in time, centered in space (FTCS) finite difference approximation applied to (35) results in an unconditionally unstable scheme.

c.

Show that the upwind scheme inherently includes a numerical diffusion with a diffusion coefficients given by

$$\frac{1}{2}|u_0|\Delta x(1-C) \tag{37}$$

where C is the Courant number given in (36).

d.

Initially we let

$$\psi(x,0) = \psi_0 e^{-\left(\frac{x}{\sigma}\right)^2} \quad ; \quad \forall x \in [-\infty, \infty], \tag{38}$$

at time $t = 0$. Here ψ_0 is the maximum tracer concentration and σ is a measure of the width of the bell. Thus the larger σ is, the wider the bell is.

Under these circumstances show that the analytic solution to (35) is

$$\psi(x,t) = \psi_0 e^{-\left(\frac{x-u_0 t}{\sigma}\right)^2}. \tag{39}$$

Part 2: Numerical solutions

We now solve (35) numerically. In this we use (38) as the initial condition. However, as is obvious, we have to limit our domain to a finite domain, say $x \in [-L, L]$. We note that these boundaries are artificial and hence that the governing equation (35) are valid at the two boundaries $x = -L$ and $x = L$ as well as in the interior domain $x \in \langle -L, L\rangle$. These boundaries are therefore open boundaries in the sense that the solution is unimpeded there.

In accord with the analytic solution we note that the peak of the bell at the times $t_c^m = 2mL/|u_0|$ is positioned at $x = 2mL$, where $m = 0(1)N$. Hence if we map the analytic solution for $x \in [(2n-1)L, (2n+1)L]$; $n = 1, 2, \ldots$ onto $x \in [-L, L]$ the solutions are all on top of each other. Numerically we mimic this by imposing a so called cyclic condition requiring

$$\psi(x,t) = \psi(x + 2L, t). \tag{40}$$

Thus whatever leaves the interior domain at $x = L$ then immediately shows up at the left hand boundary $x = -L$.

In the following we will investigate the evolution in time of two initial Gaussian bell functions. The first is a wide bell with $\sigma_1 = \frac{2L}{10}$, while the second is a narrow bell with $\sigma_2 = \frac{2L}{1000}$. For both cases we let $\Delta x = \frac{1}{10}\sigma_1$, which properly resolves the wide bell, but not the narrow bell. Furthermore we let $L = 50$ km.

e.

Let $x_j = -L + (j-1)\Delta x$ for $j = 1(1)J + 1$. Show that

$$J = \frac{2L}{\Delta x}. \tag{41}$$

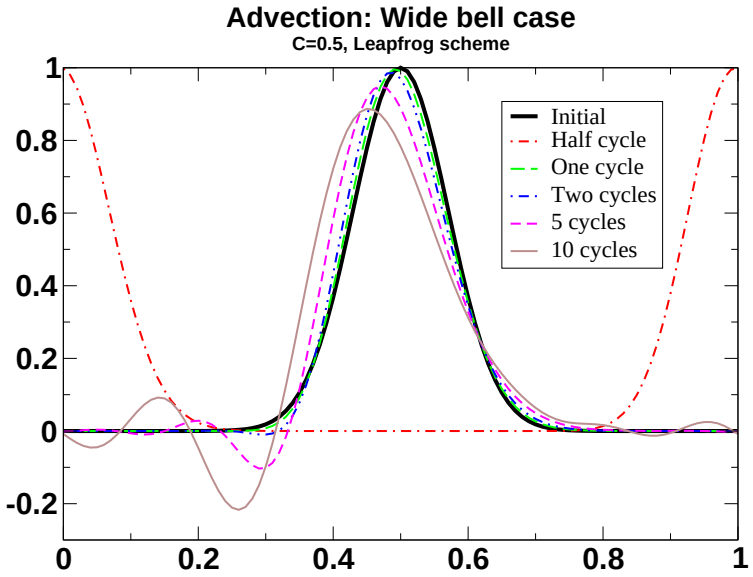

Figure 4: Displayed is the solution for the wide bell case using the leapfrog scheme with a Courant number equal one half (C=0.5).

f.

Furthermore, show that the numerical analogue of the cyclic boundary condition (40) is

$$\psi^n_{J+j} = \psi^n_j \quad \text{for} \quad j = 1(1)\cdots, \tag{42}$$

and that the numerical analogue of the initial condition (38) is

$$\psi^0_j = \psi_0 e^{-\left[\frac{-L+(j-1)\Delta x}{\sigma}\right]^2} \quad \text{for} \quad j = 1(1)J+1. \tag{43}$$

g.

Solve (35) using the leapfrog, upwind/upstream and Lax-Wendroff schemes subject to the conditions (42) and (43). Stop the computations after 10 cycles, that is, when the peak of the bell has traversed ten times the distance $2L$. Do one experiment with the Courant number $C = 0.5$ and another with $C = 1$. Please also feel free to experiment with other Courant numbers $\frac{1}{2} < C < 1$ and other space increments Δx. Plot the solution after 1/2, 1, 2, 5 and 10 cycles together with the initial tracer distribution for each of the two Courant number values. Lump the plots for the concentration as a function of distance into one plot for each scheme, that is, six curves on each plot, as exemplified in Figure 4.

h.

Discuss the solutions based on the plots. What characterizes the solution as it evolves in time? Which of the solutions are diffusive and which are dispersive? What are the characteristics of these processes?

i.

Use the Semi-Lagrange method to explain why the upstream (upwind) scheme is perfect when $C = 1$. Also show that under these circumstances all higher order numerical "diffusion" terms for the upwind scheme are zero.

6 Problem set: Flux correction methods

We continue to consider numerical solutions to the advection equation (35) in which the advection speed is not necessarily a constant. Writing the advection equation in flux form we get

$$\partial_t \theta + \partial_x (u\theta) = 0 \tag{44}$$

where θ is the tracer fraction.

To solve (44) we consider a non-staggered grid as shown in Figure 5 with a grid distance of Δx. Furthermore we consider using the scheme

$$\theta_j^{n+1} = \theta_j^n - \left(F_j^n - F_{j-1}^n\right), \tag{45}$$

where F_j^n is given by

$$F_j^n = \frac{1}{2}\left[\left(u_j^n + |u_j^n|\right)\theta_j^n + \left(u_{j+1}^n - |u_{j+1}^n|\right)\theta_{j+1}^n\right]\frac{\Delta t}{\Delta x}. \tag{46}$$

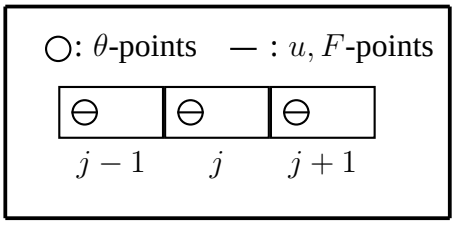

Figure 5: Displayed is the cell structure of lattice A of *Mesinger and Arakawa* (1976) (non-staggered) in one space dimension. The circels are associated with θ-points, while the horizontal bar is associated with u- and F-points within the same cells counted using the counter j. The distance between two adjacent θ-points (and hence also u- and F-points) are Δx.

Part 1:

a.

Show that (45) is, a first order scheme in time and space[4].

b.

Show that the scheme (45) is stable under the condition

$$\max_{j,n}\left(\frac{u_j^n \Delta t}{\Delta x}\right) \leq 1, \tag{47}$$

where we have assumed that the velocity is slowly varying in space, that is, $u_{j+1}^n \approx u_j^n$.

[4]Hint: Do the analysis for $u_j^n \geq 0$ and $u_j^n < 0$ separately.

c.

We now assume that $u = u_0$ is a constant. Under these circumstances show that the scheme (45) has a numerical diffusion with a diffusion coefficient κ^* given by

$$\kappa^* = \frac{1}{2}|u_0|(\Delta x - |u_0|\Delta t). \tag{48}$$

Part 2:

We observe that there are two integration constants, one in time and one in space. Thus to solve (44) we need to specify one boundary condition in time (the initial condition) and one boundary conditions in space.

In what follows we assume that the initial tracer distribution is a Gaussian bell given by

$$\theta|_{t=0} = \theta_0 e^{-\left(\frac{2x-L}{\sigma}\right)^2} \tag{49}$$

where θ_0 is the maximum tracer fraction, σ is a measure of the width of the Gaussian bell and L is a length specifying the position in space for which the tracer contration is maximum ($x = L/2$). As in Computer Problem Set 3 on page 12 we assume that the tracer distribution is cyclic within the range $x \in [0, L]$.

d.

We will now solve (44) for $x \in \langle 0, L]$ numerically using the scheme (45) within the time range $t \in \langle 0, \infty \rangle$ assuming that the initial condition (49) prevails for $t = 0$. Let $\sigma = L/10$ and the space increment be $\Delta x = \sigma/10$, $\theta_0 = 10$ºC, $u_0 = 1$m/s and $t_n = n\Delta t$ where n is the time counter and Δt is the time step. Furthermore let $L =$50km. Plot the results after 0 (initial distribution), 5, 10, 15, 20, and 25 cycles.

Describe and discuss what you observe by comparing the evolution of the tracer distribution with the initial tracer distribution. Explain what happens.

e.

According to *Smolarkiewicz* (1983) it is possible to counteract the inherent numerical diffusion in the scheme (45) by adding a correction term to (44), that is, by solving the equation

$$\partial_t \theta + \partial_x[(u + u^*)\theta] = 0. \tag{50}$$

rather than (44). The velocity u^* is the so called *anti-diffusive velocity* defined by

$$u^* = \kappa \begin{cases} \partial_x \theta / \theta & , \quad \theta > 0 \\ 0 & , \quad \theta \leq 0 \end{cases} . \tag{51}$$

Smolarkiewicz named his method the Multidimensional Positive Definite Advection Transport Algorithm or MPDATA method.

Solve (50) using the MPDATA method, that is, the predictor-corrector method. Use first the iterative method with at least two steps, then the simple method of scaling the anti-diffusive velocity. Let the parameters and initial condition be as in Part 1, item **d.**. When scaling use a scaling factor of $S_c = 1.3$. When computing the anti-diffusive velocity use a centered in space finite difference approximation, and ensure that you add, as suggested by *Smolarkiewicz* (1983), a small number $\epsilon = 10^{-15}$ in the denominator.

f.

Why do we have to add the small number ϵ to the denominator?

g.

Make experiments varying the scaling factor S_c. Try out other finite difference approximations to the anti-diffusive velocity. Discuss the results.

7 Problem set: Geostrophic Adjustment

One of the most important and strongest balances in the atmosphere and ocean, confirmed over and over again by observations, is geostrophy. When the fluid motion is in geostrophic balance we have a balance between the Coriolis acceleration and the pressure forcing, that is,

$$f\mathbf{k}\times\mathbf{u}_g = -\frac{1}{\rho_0}\nabla_H p, \quad \text{or} \quad v_g = \frac{1}{\rho_0 f}\partial_x p, \quad u_g = -\frac{1}{\rho_0 f}\partial_y p, \tag{52}$$

where $f = 2\Omega\sin\phi$ is the Coriolis parameter, $\mathbf{k}$ is the unit vector along the vertical z-axis, $\mathbf{u}_g$ is the (horizontal) geostrophic velocity with components u_g, v_g along the x-axis and y-axis, respectively, ρ_0 is the density, $\nabla_H = \mathbf{i}\partial_x + \mathbf{j}\partial_y$ is the horizontal component of the three-dimensional del-operator, and p is pressure. Note that (52) contains three unknowns, namely p, u_g, and v_g, but only two equations. Hence the solution is undetermined. Only by specifying one of them, say the pressure p, can we find the two other variables.

A fundamental question is therefore how the atmosphere and ocean actually adjust from an unbalanced state to one in geostrophic balance under gravity. This problem, coined geostrophic adjustment (under gravity), was first raised by Carl Gustav Rossby[5] back in the 1930s (*Rossby*, 1937, 1938), and is nicely summarized by *Blumen* (1972) and (*Gill*, 1982, Chapter 7, Section 7.2, page 191). It is the background for this computer problem.

As usual we make the problem as simple as possible, but no simpler. Thus, we consider the one-dimensional (1-D) shallow water equations for this purpose. It conveniently serves the purpose of illustrating the wave-modes of the solution, the role of initial conditions and the use of an open boundary condition (FRS).

We recall that the shallow water equations assumes a hydrostatic balance and hence that $p = \rho_0 g h$, where h is the geopotential height. Thus the governing equations, inherently non-linear, are

$$\partial_t h = -\nabla_H\cdot(h\mathbf{u}), \tag{53}$$

$$\partial_t \mathbf{u} = -f\mathbf{k}\times\mathbf{u} - \mathbf{u}\cdot\nabla_H\mathbf{u} - g\nabla_H h, \tag{54}$$

where the Coriolis parameter is $f = 1.26\cdot 10^{-4}\mathrm{s}^{-1}$ (corresponding to its value at 60^oN). As is common we may regard h as the geopotential height of a pressure surface in the atmosphere and as the depth of a water column in the ocean. The equilibrium height of h in the atmosphere is associated with a pressure surface of ≈ 900hPa, while the equilibrium depth in the ocean is commonly ≈ 1km.

[5]Carl-Gustaf Arvid Rossby (1898 - 1957) was a Swedish-U.S. meteorologist who pioneered explaining the large-scale motions of the atmosphere in terms of fluid mechanics. Rossby came into meteorology and oceanography while studying under Vilhelm Bjerknes in Bergen in 1919, where Bjerknes' group was developing the concept of a polar front (the Bergen School of Meteorology). His name is associated with various quantities and phenomena in meteorology and oceanography, e.g., the Rossby number, Rossby's radius of deformation, and Rossby waves.

Part 1:

a.

Show that by introducing $\mathbf{U} = h\mathbf{u}$ and $h = h$ as new variables then (53) and (54) become

$$\partial_t h = -\nabla_H \cdot \mathbf{U}, \tag{55}$$

$$\partial_t \mathbf{U} = -f\mathbf{k} \times \mathbf{U} - \nabla_H \cdot \left(\frac{\mathbf{U}\mathbf{U}}{h}\right) - \frac{1}{2} g \nabla_H h^2. \tag{56}$$

b.

Show that (53) and (54) may be combined to yield the vorticity equation

$$(\partial_t + \mathbf{u} \cdot \nabla_H) P_v = 0, \tag{57}$$

where P_v is the potential vorticity defined as

$$P_v = \frac{\zeta + f}{h}, \tag{58}$$

where in turn $\zeta = \mathbf{k} \cdot \nabla_H \times \mathbf{u}$ is the relative vorticity.

c.

Let us assume that the motion is independent of y ($\partial_y = 0$). Show that under these circumstances (53) and (54) reduces to

$$\partial_t h = -u\partial_x h - h\partial_x u, \tag{59}$$

$$\partial_t u = fv - u\partial_x u - g\partial_x h, \tag{60}$$

$$\partial_t v = -fu - u\partial_x v, \tag{61}$$

and show that the steady state solution to (59) - (61) then is one in geostrophic balance and given by

$$u = 0 \quad \text{and} \quad v = \frac{g}{f}\partial_x h. \tag{62}$$

d.

Utilize (57) and (62) to show that the steady state solution to (59) - (61) is a solution to the ordinary differential equation

$$\partial_x^2 h - \frac{f P_{v0}}{g} h = -\frac{f^2}{g}, \tag{63}$$

where $P_{v0} = P_{v0}(x)$ is the initial distribution of the potential vorticity.

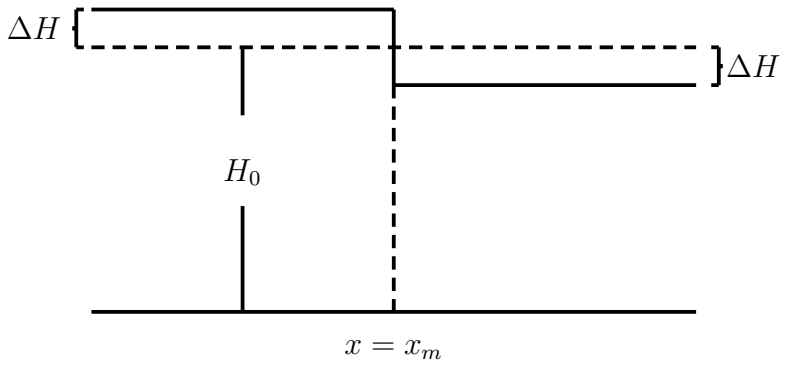

Figure 6: Depicted is the initial geopotential height according to (64).

e.

Let us assume that the initial condition is one at rest, and that the geopotential height is given by a Heaviside function, that is,

$$u = v = 0, \quad \text{and} \quad h = H_0 - \text{sgn}(x - x_m)\Delta H \quad \text{at} \quad t = 0, \forall x \tag{64}$$

where $\text{sgn}(\psi) = +1$ if $\psi \geq 0$ and $\text{sgn}(\psi) = -1$ if $\psi < 0$ (Figure 6). Show that under these circumstances the solution to (63) is

$$h = H_0 + \Delta H \begin{cases} 1 - \frac{2\lambda_-}{\lambda_- + \lambda_+} e^{\frac{x - x_m}{\lambda_-}} & \text{if } x < x_m \\ -1 + \frac{2\lambda_+}{\lambda_- + \lambda_+} e^{-\frac{x - x_m}{\lambda_+}} & \text{if } x \geq x_m \end{cases} . \tag{65}$$

where $\lambda_\pm = \frac{1}{f}\sqrt{g(H_0 \mp \Delta H)}$ is Rossby's deformation radius, and where $H_0 = 1000$ m, $\Delta H = 15$ m, $u_g = 0$ ms^{-1}, and $x_m = D/2$ is the middle point of the domain of length D. Is the height anomaly $h - H_0$ negative or positive at $x = x_m$? Discuss the solution.

f.

If you were to solve the system (59) - (61), how many boundary and initial conditions do you have at your disposal? Explain how you derived the number of conditions.

Part 2:

We will solve the system (59) - (61) using numerical methods for a limited domain $x \in \langle 0, D \rangle$. To this end we need boundary conditions at $x = 0, D$ and initial conditions at time $t = 0$. We assume that the motion is started from one at rest and where the geopotential height (or ocean surface) is given by (64).

g.

Construct a CTCS (leapfraog) scheme to solve (59) - (61). Describe in some detail how you derive the various terms. Explain your choices. Add a filter to remove the two gridlength noise (cf. the Lecture Notes).

h.

Is the CTCS scheme consistent? Derive under what condition(s) the scheme you have constructed is stable[6]. How long time step Δt may be used?

i.

Construct a Semi-Lagrange scheme to solve (59) - (61). Describe in some detail how you derive the finite difference analogue and the choices you make.

j.

Let the grid length be $\Delta x = 100$km and $D = 62\Delta x$ and solve the above equations numerically using first the leapfrag (CTCS) scheme and then the Semi-Lagrange scheme you have constructed for the domain $x \in \langle 0, D \rangle$. Assume that the variables u, v, and h retain their initial values at the boundaries $x = 0$ and $x = D$.

Plot h hourly, including the initial time, for the first 10 hours. Plot also the solution after 300 hours. Discuss the solutions. Try to make a movie spanning $t \in [0, 300]$hrs. What kind of waves do you observe?

k.

Repeat the above computation using the the FRS method to relax the inner solution towards the externally specified values $(\hat{u}, \hat{v}, \hat{h}) = (0, 0, H_0 + \Delta H)$ at $x = 0$ and $(\hat{u}, \hat{v}, \hat{h}) = (0, 0, H_0 - \Delta H)$ at $x = D$. Let the buffer zone be seven points wide where the relaxation parameter λ_j is as given in Table 2.

Compare the two solutions, for instance by plotting the difference between them, and discuss any differences. Also compare the two solutions to the steady state solution you derived in item **e**. Explain and discuss any differences you observe.

l.

Compute the geostrophic component of the velocity

$$v_g = \frac{g}{f}\partial_x h \tag{66}$$

[6]Hint: We always neglect the non-linear terms when performing the stability analysis.

j	λ_j	j
1	1.0	j_{max}
2	0.69	$j_{max} - 1$
3	0.44	$j_{max} - 2$
4	0.25	$j_{max} - 3$
5	0.11	$j_{max} - 4$
6	0.03	$j_{max} - 5$
7	0.0	$j_{max} - 6$

Table 2: Values of the relaxation parameter used in Part 2, item **j**. The left-hand column refers to the j numbers in the left-hand FRS zone, where $x = 0$ corresponds to $j = 1$. The right-hand column refers to the right-hand FRS zone where $x = D$ corresponds to $j = j_{max}$.

using the solution for h at $t = 6$ hours. Compare v_g and v at $t = 10$ hours and describe and discuss what you observe. What do you think have happened?

m.

Finally, replace the initial condition and boundary conditions for v in (64) by one in geostrophic balance, that is,

$$v = \frac{g}{f}\partial_x h_s. \tag{67}$$

where h_s is the steady state solution displayed by (65). Redo the computations and discuss the solutions you get.

8 Problem set: Planetary waves

One of the most important and strongest balances in the atmosphere and ocean, confirmed over and over again by observations, is geostrophy. When the fluid motion is in geostrophic balance we have a balance between the Coriolis acceleration and the pressure forcing, that is,

$$f\mathbf{k}\times\mathbf{u}_g = -\frac{1}{\rho_0}\nabla_H p, \quad \text{or} \quad v_g = \frac{1}{\rho_0 f}\partial_x p, \quad u_g = -\frac{1}{\rho_0 f}\partial_y p, \tag{68}$$

where $f = 2\Omega\sin\phi$ is the Coriolis parameter, $\mathbf{k}$ is the unit vector along the vertical z-axis, $\mathbf{u}_g$ is the (horizontal) geostrophic velocity with components u_g, v_g along the x-axis and y-axis, respectively, ρ_0 is the density, $\nabla_H = \mathbf{i}\partial_x + \mathbf{j}\partial_y$ is the horizontal component of the three-dimensional del-operator, and p is pressure. Note that (68) contains three unknowns, namely p, u_g, and v_g, but only two equations. Hence the system is underdetermined. Only by specifying one of them, say the pressure p, can we find the two other variables.

A fundamental question is therefore how the atmosphere and ocean actually adjust from an unbalanced state to one in geostrophic balance under gravity. This problem, coined geostrophic adjustment (under gravity), was first raised by Carl Gustav Rossby[7] back in the 1930s (*Rossby*, 1937, 1938), and is the background for this computer problem. As usual we make the problem as simple as possible, but no simpler. Thus, we consider the one-dimensional (1-D) shallow water equations for this purpose. It also conveniently serves the purpose of illustrating solution modes, the role of initial conditions and the use of an open boundary condition (FRS).

We recall that the shallow water equations assumes a hydrostatic balance and hence that $p = \rho_0 g h$, where h is the geopotential height. Thus the governing equations, inherently nonlinear, are

$$\partial_t h = -\nabla_H\cdot(h\mathbf{u}), \tag{69}$$

$$\partial_t \mathbf{u} = -f\mathbf{k}\times\mathbf{u} - \mathbf{u}\cdot\nabla_H\mathbf{u} - g\nabla_H h, \tag{70}$$

where the Coriolis parameter is $f = 1.26\cdot 10^{-4}\text{s}^{-1}$ (corresponding to its value at 60^{o}N). As is common we may regard h as the geopotential height of a pressure surface in the atmosphere and as the depth of a water column in the ocean. The equilibrium height of h in the atmosphere is associated with a pressure surface of ≈ 900hPa, while the equilibrium depth in the ocean is commonly ≈ 1km.

[7] Carl-Gustaf Arvid Rossby (1898 - 1957) was a Swedish-U.S. meteorologist who pioneered explaining the large-scale motions of the atmosphere in terms of fluid mechanics. Rossby came into meteorology and oceanography while studying under Vilhelm Bjerknes in Bergen in 1919, where Bjerknes' group was developing the concept of a polar front (the Bergen School of Meteorology). His name is associated with various quantities and phenomena in meteorology and oceanography, e.g., the Rossby number, Rossby's radius of deformation, and Rossby waves.

Part 1:

a.

Show that by introducing $\mathbf{U} = h\mathbf{u}$ and $h = h$ as new variables (69) and (70) become

$$\partial_t h = -\nabla_H \cdot \mathbf{U}, \tag{71}$$

$$\partial_t \mathbf{U} = -f\mathbf{k} \times \mathbf{U} - \nabla_H \cdot \left(\frac{\mathbf{UU}}{h}\right) - \frac{1}{2} g \nabla_H h^2. \tag{72}$$

b.

Show that (71) and (72) may be combined to yield the vorticity equation

$$(\partial_t + \mathbf{u} \cdot \nabla_H) P_v = 0, \tag{73}$$

where P_v is the potential vorticity defined as

$$P_v = \frac{\zeta + f}{h}, \tag{74}$$

where in turn $\zeta = \mathbf{k} \cdot \nabla_H \times \mathbf{u}$ is the vorticity.

c.

Let us assume that the motion is independent of y ($\partial_y = 0$). Show that under these circumstances (69) and (70) reduces to

$$\partial_t h = -u\partial_x h - h\partial_x u, \tag{75}$$

$$\partial_t u = fv - u\partial_x u - g\partial_x h, \tag{76}$$

$$\partial_t v = -fu - u\partial_x v, \tag{77}$$

and (71) and (72) reduces to

$$\partial_t h = -\partial_x U, \tag{78}$$

$$\partial_t U = fV - \partial_x \left(\frac{U^2}{h} + \frac{1}{2} g h^2\right) \tag{79}$$

$$\partial_t V = -fU - \partial_x \left(\frac{UV}{h}\right). \tag{80}$$

Part 2:

We will solve the shallow water equations using numerical methods for a limited domain $x \in \langle 0, L \rangle$. To this end we need boundary conditions at $x = 0, L$ and initial conditions at time $t = 0$.

We assume that the motion is started from one at rest in which the geopotential height (or ocean surface) is perturbed. Thus the initial conditions are

$$u = v = 0, \quad \text{and} \quad h(x,t) = H_0 + Ae^{-\left(\frac{x-x_m}{\sigma}\right)^2} \tag{81}$$

where $H_0 = 1000$ m, $A = 15$ m, $x_m = L/2$ is the middle point of the domain, and σ is a measure of the width of the Gaussian bell.

d.

How many boundary and initial conditions are you allowed to specify when solving the system (75) - (77)? Explain how you derived the number of conditions.

e.

Under items $\mathbf{g}$. and $\mathbf{h}$. you are asked to solve the shallow water equations using either the system (75) - (77) or the system (78) - (80). To this end adopt a CTCS scheme, and describe here in detail how you derive the finite difference approximation to the various terms. Explain your choices.

f.

Under what conditions is the scheme stable? Describe in detail how you analyzed the stability and the consistency of the scheme[8]. How long time step Δt can be used? Explain your choice.

g.

Solve either the system (75) - (77) or the system (78) - (80) using the CTCS scheme you have constructed for the domain $x \in \langle 0, L\rangle$. Assume that the variables retain their initial values at the boundaries $x = 0$ and $x = L$. Further, let the grid length be $\Delta x = 100$km, $L = 62\Delta x$ and $\sigma = 5\Delta x$.

Plot h at time $t = 0$, 1.5, 3.0, 4.5, 6.0 and 10.0 hours. Discuss the solution. Try to make a movie spanning $t \in [0, 10]$hrs. What kind of waves do you observe?

h.

Repeat the above computation using the the FRS method relaxing the inner solution towards an externally specified solution given by $(\hat{u}, \hat{v}, \hat{h}) = (0, 0, H_0)$. Let the FRS or buffer zone be seven points wide within which the relaxation parameter λ_j varies in the two FRS zones as given in Table 3.

Compare the solution to the one you obtained performing the computation in item **g.**, for instance by plotting the difference between them. Explain and discuss any differences you observe.

[8] Hint: Neglect the non-linear terms when performing the stability analysis.

j	λ_j	j
1	1.0	j_{max}
2	0.69	$j_{max} - 1$
3	0.44	$j_{max} - 2$
4	0.25	$j_{max} - 3$
5	0.11	$j_{max} - 4$
6	0.03	$j_{max} - 5$
7	0.0	$j_{max} - 6$

Table 3: Values of the relaxation parameter used in Part 2.

i.

Compute the geostrophic component of the velocity

$$v_g = \frac{g}{f}\partial_x h \tag{82}$$

using the solution for h at $t = 6$ hours. Compare v_g and v at $t = 6.0$ hours and describe and discuss what you observe. What do you think have happened?

j.

Finally, replace the initial condition for v in (81) by

$$v = \frac{g}{f}\partial_x h. \tag{83}$$

and repeat the computation of item **h.** using (83) as initial condition. Discuss the solution by comparing it to the solution obtained through item **h.** above.

9 Problem set: Rossby waves

The response of the atmosphere an ocean consists in many cases of various types of waves. One important distinct type of wave response is the barotropic Rossby wave *LaCasce* (2009). These waves are unique in the sense that their phase velocity is westward while their group velocity is eastward. Since the energy of the waves propagates with the group velocity it implies that the waves tend to die out as they propagate westward. Another unique feature is that the phase velocity or wave speed depends on the rate at which the Earths rotation changes with latitude. Hence the wave speed decreases with latitude. Consequently the Rossby waves are hard to observe at high latitudes.

The equation governing these waves is derived from the linear, barotropic shallow water equation, that is,

$$\partial_t \mathbf{u} + f\mathbf{k} \times \mathbf{u} = -\nabla_H \phi, \tag{84}$$

$$\partial_t \phi + c_0^2 \nabla_H \cdot \mathbf{u} = 0, \tag{85}$$

with the additional assumption that the motion is effectively divergence free. Thus we get

$$\partial_t \zeta + \beta \partial_x \psi = 0, \tag{86}$$

where ψ is the streamfunction, that is, $\mathbf{u} = \mathbf{k} \times \nabla_H \psi$ and $\zeta = \mathbf{k} \cdot \nabla_H \times \mathbf{u}$ is the vorticity. The constant $\beta = 2 \cdot 10^{-11}(ms)^{-1}$ represents the first order effect of the impact of the change in the Earth's rotation rate with latitude, that is, the first derivative in a Taylor series expansion of the Coriolis parameter f with respect to the latitude y, viz.,

$$f(y) = f|_{y=y_0} + \beta(y - y_0) + O\left([y - y_0]^2\right) \quad \text{where} \quad \beta = \partial_y f|_{y=y_0}. \tag{87}$$

Here we will solve the one-dimensional version of (86) by numerical means. Thus the governing equation we solve is

$$\partial_t \left(\partial_x^2 \psi\right) + \beta \partial_x \psi = 0. \tag{88}$$

Part 1: Analysis

a.

Show that (88) follows from (84) and (85) and discuss under the assumption under which it is correct. For instance, what physics are neglected?

b.

Show that the wave solution

$$\psi(x,t) = Re\left\{Ae^{i\alpha(x-ct)}\right\} \tag{89}$$

is a is solution to (88), where c is the phase speed and α is the wavenumber. Note that A is an imaginary number so that the solution may be written

$$\psi = A_r \cos\alpha(x - ct) - A_i \sin\alpha(x - ct), \tag{90}$$

where $A_r = Re\{A\}$ is the real part of A and $A_i = Im\{A\}$ is the imaginary part of A.

c.

Show that the phase speed c of the Rossby wave is

$$c = -\frac{\beta}{\alpha^2}. \tag{91}$$

and that the group velocity, c_g is

$$c_g = -c. \tag{92}$$

d.

How many boundary/initial conditions must be specified in order to solve (88)?

e.

Before we solve (88) numerically within the finite domain $x \in< 0, L >$ we make it non-dimensional. Show that by choosing a typical time scale given by

$$T = \frac{1}{\beta L}, \tag{93}$$

the non-dimensional version of (88) becomes

$$\partial_t^* \left(\partial_{x^*}^2 \psi^*\right) + \partial_x^* \psi^* = 0, \quad ; \quad \forall x^* \in< 0, 1 >, \tag{94}$$

or

$$\partial_t \left(\partial_x^2 \psi\right) + \partial_x \psi = 0, \quad ; \quad \forall x \in< 0, 1 >, \tag{95}$$

where we have dropped the stars for clarity.

Part 2: Numerical solutions

We will experiment with three different initial distributions for the streamfunction, namely a simple wave, a more complex wave and a Gaussian distribution, that is,

$$\psi|_{t=0} = \begin{cases} \sin \alpha x & \text{the simple wave} \\ \sin \alpha x \cos \alpha x & \text{more complex wave} \\ e^{-\left(\frac{x}{\sigma}\right)^2} & \text{Gaussian distribution} \end{cases} \tag{96}$$

where α is a finite, non-dimensional wavenumber different from zero and $\sigma = 0.001$ is a measure of the (narrow) width of the Gaussian bell. Let $\alpha = 2m\pi$, $m = 2$ for the simple and more complex wave. We note that the latter makes $\psi = 0$ at $x = 0$ and $x = 1$ at time $t = 0$.

To solve (95) we first split it in two, that is,

$$\partial_t \zeta + \partial_x \psi = 0, \tag{97}$$

and

$$\partial_x^2 \psi = \zeta, \tag{98}$$

where ζ is the non-dimensional vorticity. We note that to solve (97) and (98) properly the space increment Δx must be chosen small enough to resolve the dominant waves given in (96). Next the time increment Δt must be chosen so that the stability condition is satisfied, if any.

d.

Show that for a monochromatic wave the non-dimensional wave speed is

$$c = -\frac{1}{\alpha^2}. \tag{99}$$

where α is the non-dimensional wave number of the monochromatic wave.

e.

Construct a CTCS scheme for (97) and (98) that results in an explicit, consistent, neutral and conditionally stable scheme, and derive the condition for stability.

f.

Solve (97) and (98) within the domain $x \in < 0, 1 >$ using the CTCS scheme constructed under subsection **e.** using the three initial conditions (96) and appropriate boundary condition. Explain why two boundary conditions are needed in space and show that to mimic an infinite plane one of them have to be the periodic boundary condition, that is,

$$\psi(x, t) = \psi(x + 1, t). \tag{100}$$

Let the second boundary condition be the radiation condition, that is,

$$\partial_t \psi + c\partial_x \psi = 0 \quad \text{at} \quad x = 0, \tag{101}$$

where c is a non-dimensional wave speed given. Note that for the two monochromatic waves in (96) the non-dimensional wave speed c can be calculated using (99). Note that c is not specified when using the initial Gauss distribution. In this case c will be a function of time and must be calculated by numerical means for each time step[9].

g.

Plot the solution in a Hovmöller diagram in the x, t space with x along the horizontal axis and t along the vertical axis. Verify your numerical solution by reading off the wave speed from the Hovmöller diagram and check it against the true wave speed given in (99).

[9] Hint: Use the condition $\partial_t \zeta + c\partial_x \zeta = 0$ to calculate c at the left-hand boundary.

h.

Solve (97) and (98) using the CTCS scheme but this time within a closed domain. Show first that a closed domain requires that

$$\psi = 0 \quad \text{at} \quad x = 0 \quad \text{and} \quad x = 1. \tag{102}$$

Plot the solution as a function of x, t using a Hovmöller diagram as in item **g**. Discuss the differences between the solutions with open and closed boundaries respectively by comparing the two Hovmöller diagrams.

10 Problem set: Storm surges

We consider below the storm surge problem. The purpose is to gain experience in constructing numerical solutions to geophysical problems that include more than one dependent variable.

The water level of the ocean changes due to three main factors. For one it responds to the astronomical forcing which gives rise to the well known tidal phenomenon, a deterministic periodic response in the water level. Next the water level in the ocean changes due to the forcing exerted by the atmosphere through wind stress and sea level pressure. This phenomenon is referred to as the storm surge response and its associated water level change is referred to as the storm surge. From time to time the joint occurrence of high tides and high storm surges can lead to devastating high water levels even along the Norwegian coast. One such example is from mid October 1987 where the water level in Oslo Harbor reached 1.96 meters above normal sea level. More examples are given in *Gjevik* (2009). Finally the water level of the ocean may change due to expansion by heating. This latter is a concern with regard to climate change in that the water level rises under global warming.

To secure life and property many countries early on developed forecasts services for tides and storm surges. As numerical ocean models were developed in the late 1960s and early 1970s one of the first models that were developed was in fact numerical models to forecast storm surges and tides. For instance the National Oceanography Center, Liverpool, UK (formerly the Proudman Oceanographic Laboratory) was founded in the late 1960s to forecast tides and storm surges in British waters, and has since then been one of the leading institutions within this field. Since the late 1970s and early 1980s also the Norwegian Meteorological Institute has developed numerical models to forecast sea level changes due to storm surges and tides using numerical models developed through the work of *Gjevik and Røed* (1976), *Martinsen et al.* (1979) and *Røed* (1979).

Many of the earlier studies of storm surges, including those just referenced, have shown that the storm surge is mainly a barotropic response. To construct a storm surge model we may therefore use an ocean in which we assume the density to be constant in time and space. The equations therefore reduce to the well known shallow water equations. Let

$$\mathbf{U}(x,y,t) = \int_{-H(x,y)}^{\zeta(x,y,t)} \mathbf{u}(x,y,z,t)dz, \tag{103}$$

with components (U,V) along the x,y-axes, respectively, be the transport of water in a water column of depth $h = H + \zeta$ where ζ is the sea level deviation away from the equilibrium depth H (see Figure 7). Then the shallow water equations are

$$\partial_t \mathbf{U} + \nabla_H \cdot \left(h^{-1}\mathbf{U}\mathbf{U}\right) + f\mathbf{k}\times\mathbf{U} = -gh\nabla_H\zeta + \rho_0^{-1}(\boldsymbol{\tau}_s - \boldsymbol{\tau}_b), \tag{104}$$

$$\partial_t h + \nabla_H \cdot \mathbf{U} = 0. \tag{105}$$

where $\boldsymbol{\tau}_s$ and $\boldsymbol{\tau}_b$ are respectively the wind and bottom stresses with components (τ_s^x, τ_s^y) and (τ_b^x, τ_b^y), g is the gravitational acceleration and ρ_0 is the (uniform in time and space) density. The Coriolis parameter is $f = 2\Omega\sin\phi$ where Ω is the Earth's rotation rate and ϕ is the latitude.

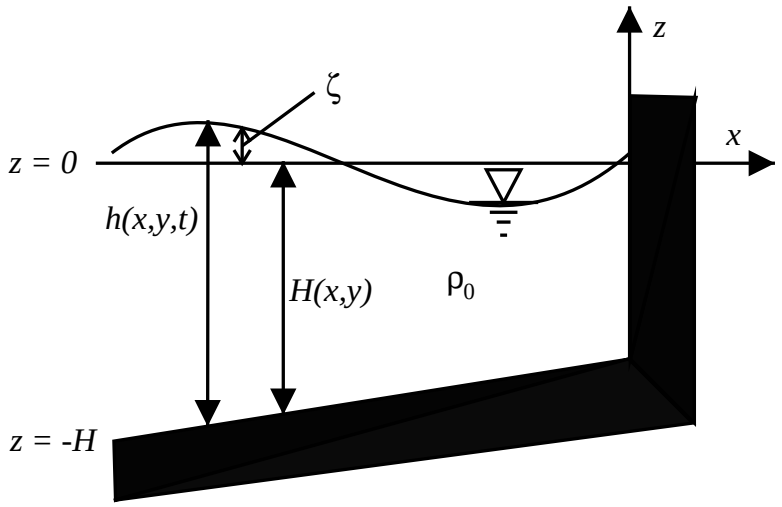

Figure 7: Sketch of a storm surge model along a straight coast conveniently showing some of the notation used.

We observe that the second term on the left-hand side and the first term on right-hand side of (104) are non-linear terms. The main effect of these terms is to get the interaction of tides and storm surges correct. In many instances this effect is small, and in the remainder we will neglect them.

To make things even simpler we will also look for solution of the storm surge problem in the presence of a straight coast along the y-axis as sketched in Figure 7. Under these circumstances we may also neglect terms containing derivatives with respect to y, that is, we let $\partial_y = 0$. Thus through linearization and negligence of variations with respect to y we get from (104) and (105) that

$$\partial_t U - fV = -gH\partial_x h + \rho_0^{-1}(\tau_s^x - \tau_b^x), \tag{106}$$

$$\partial_t V + fU = \rho_0^{-1}(\tau_s^y - \tau_b^y), \tag{107}$$

$$\partial_t h + \partial_x U = 0. \tag{108}$$

It is also safe to neglect the variation with latitude in the effect of the Earth's rotation. Thus we may safely assume that the Coriolis parameter is constant in time and space. In the following we will also assume that changes in the equilibrium depth are so small that H to a good approximation can be considered as being constant as well, that is, we let $H = H_0$ where H_0 is a constant.

In summary (106) - (108) allow us to investigate linear, analytic and numerical solution to the storm surge problem along a straight coast assuming a flat bottom. To this end we will assume that the initial condition is an ocean at rest and in equilibrium. Furthermore we will assume that the coast is impermeable, that is, the natural boundary condition there is no flow through the coast. Otherwise the domain is unlimited, and hence we assume that far away from the coast the solution approaches the Ekman solution ($\partial_x = 0$).

Part 1:

We first look for analytic solution to (106) - (108) so as to be able to verify our numerical solutions (Part 2 below). However, even this simple system is hard to solve analytically. So we will simplify the problem even further. Nevertheless, we may still use it for verification purposes.

a.

Show that (106) - (108) follows by linearizing (104) and (105) under the assumption that changes in the equilibrium depth H are insignificant and that $|\mathbf{U}|^2 \ll |\mathbf{U}|$.

b.

Let the cost be located at $x = 0$ with the ocean extending infinitely in the negative x direction. Explain why the Ekman solution[10] is the natural open boundary condition to use there. Show that mathematically the condition is tantamount to

$$h = H \quad \text{or} \quad \partial_x h = 0 \quad \text{at} \quad x \to -\infty \quad \forall t. \tag{109}$$

Show also that the condition of no flow through the coast at $x = 0$ is

$$U = 0 \quad \text{at} \quad x = 0 \quad \forall t. \tag{110}$$

and that the initial condition may be formulated as

$$U = V = 0, \quad h = H_0 \quad \text{at} \quad t = 0 \quad \forall x. \tag{111}$$

c.

Show that the inertial oscillations, that is, solutions that oscillates with the inertia frequency f, are avoided if we neglect the term $\partial_t U$ in (106).

d.

Let us assume that there is no bottom friction, that is, $\tau_b^x = \tau_b^y = 0$ and that there is no wind stress in the x-direction ($\tau_s^x = 0$). Show that under these assumptions, and the assumption that $\partial_t U$ is small compared to the Coriolis acceleration, the motion along the coast (in the y-direction) is in geostrophic balance. Furthermore, show that the analytic solutions to (106) through (108) under these assumptions are

$$U = U_E \left(1 - e^{\frac{x}{L_R}}\right), \tag{112}$$

$$V = ftU_E e^{\frac{x}{L_R}}, \tag{113}$$

$$h = H \left(1 + \frac{tU_E}{L_R H} e^{\frac{x}{L_R}}\right), \tag{114}$$

[10] The Ekman solution is the solution we get when solving the steady state version of (106) through (108) assuming that $\partial_x = 0$ and $\tau_b^x = \tau_b^y = 0$.

where $L_R = \sqrt{gH}/f$ is the Rossby radius of deformation and

$$U_E = \frac{\tau_s^y}{\rho_0 f}, \tag{115}$$

is the Ekman transport.

e.

To investigate the effect of bottom friction solve (106) through (108) analytically under the assumptions that $\tau_b^x = 0, \tau_b^y = \rho_0 R\frac{V}{H}$, and that the term $\partial_t U$ in (106) can be neglected[11].

f.

Plot the analytical solutions of h, U and V derived under **d.** and **e.** in a $x - t$ diagram. Such a diagram is often referred to as a Hovmöller diagram.

g.

What changes are introduced to (106) through (108) if the changes in the equilibrium depth H are significant?

Part 2:

In this part we investigate numerical solutions to (106) through (108) under the assumption that the depth is constant ($H = H_0$). Furthermore we let the parameters appearing in (106) through (108) be

$$\begin{aligned} g &= 10\text{ms}^{-1}, \quad \tau_s^x = 0, \quad \tau_s^y = 0.1\text{Pa}, \quad \rho_0 = 10^3\text{kg/m}^3, \quad f = 10^{-4}\text{s}^{-1}, \\ H_0 &= 300\text{m}, \quad \tau_b^x = \rho_0 R\frac{U}{H_0}, \quad \tau_b^y = \rho_0 R\frac{V}{H_0}, \quad R = 2.4 \cdot 10^{-3}\text{m/s}. \end{aligned}$$

if not explicitly deviated.

Since one of the spatial boundary is at $x \to -\infty$ the domain is infinite. On the computer, however, the domain has to be finite, that is, we have to stop the computations at a finite distance away from the coast, say $x = -L$. Then a boundary at $x \to -\infty$ is tantamount to saying that L is large compared to some typical dynamical length scale of the problem. We note that the boundary at $x = -L$ is an open boundary. Thus the equations (106) through (108) are still valid there, and we have to construct a condition that does not violate them.

[11] Hint: Make use of Laplace transforms.

h.

Show that the dominant length scale in this problem, in fact for all shallow water problems, is the Rossby radius of deformation L_R. Show that by assuming $L \gg L_R$ then we may safely assume that the dynamics are independent of x and hence that the natural open boundary condition is therefore to let the solution approach the Ekman solution at $x = -L$.

h.

Construct a centered in space and forward-backward in time scheme[12] on a staggered B-grid. The B-grid is the one dimensional version of lattice B of *Mesinger and Arakawa* (1976) (page 47). Thus we assume that the U- and V-points are staggered one half grid length with respect to the h-points as sketched in Fig. 8.

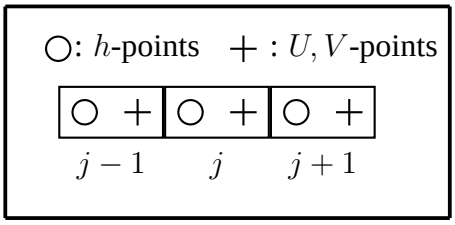

Figure 8: Displayed is the cell structure of lattice B of *Mesinger and Arakawa* (1976) in one space dimension. The circels are associated with h-points, while the horizontal bar is associated with U-points and the vertical bar with V-points within the same cells. The sketched staggering is such that the distance between adjacent h-points and U, V-points are one half grid distance apart.

i.

Show that your scheme constructed under item **h.** is neutrally stable under the condition

$$\Delta t \leq \frac{\Delta x}{c_0 \sqrt{1 + \left(\frac{\Delta x}{2L_R}\right)^2}} \tag{116}$$

using von Neumann's method[13], and where $c_0 = \sqrt{gH}$. Discuss under which the simpler condition $C \leq 1$, where $C = c_0 \Delta t / \Delta x$ is valid. Is the scheme dissipative[14]?

[12] Forward-backward in time means that as soon as one dependent variable is updated (in time) we use these values when updating the other dependent variables.

[13] Hint: When analyzing the instability neglect all forcing (stress) terms.

[14] Hint: To analyze the dissipation analyze the growth factor.

j.

Show that your scheme constructed under item **h.** is consistent.

k.

Solve the storm surge problem (106) - (108) numerically making use of your scheme constructed under item **h.** and the parameters listed including the bottom stresses. Choose Δx so that $\Delta x \ll L_R$, say $\Delta x = L_R/10$. Explain why this choice is so important.

i.

Plot the numerical solution of the dependent variables h, U and V in a Hovmöller diagram. Compare the numerical solution with those derived analytically under **d.** and **e.**. Discuss differences and similarities.

11 Problem set: Methods of characteristics applied to a non linear systems

We now solve the non-linear, rotating shallow water equations (104) on page 32 using the method of characteristics as outlined in the appendix of *Røed and O'Brien* (1983) (cf. Problem set: Storm surges on page 32). This solution method is also associated with the semi-Lagrangian method explained in the Lecture Notes (Chapter 6: "Non-linear, rotating shallow water equations"). In this we will assume that the variables are only dependent on one indepent variable in space, that is, we let $\partial_y = 0$. Furthermore we note that $\mathbf{U} = h\mathbf{u}$, and that the pressure term in (104) may be written $gh\partial_x h$ under the assumption of a constant equilibrium depth.

a.

Show that if we define $c = \sqrt{gh}$ then (104) may be rewritten to yield the compatibility equations

$$\frac{D_1^*}{dt}(u + 2c) = fv + \frac{\tau_s^x - \tau_b^x}{\rho h} \quad \text{along} \quad \frac{D_1^* x}{dt} \tag{117}$$

$$\frac{D_2^*}{dt}(u - 2c) = fv + \frac{\tau_s^x - \tau_b^x}{\rho h} \quad \text{along} \quad \frac{D_2^* x}{dt} \tag{118}$$

$$\frac{D_3^* v}{dt} = -fu + \frac{\tau_s^y - \tau_b^y}{\rho h} \quad \text{along} \quad \frac{D_3^* x}{dt} \tag{119}$$

where the operators $\frac{D_{1,2,3}^*}{dt}$ are defined as

$$\frac{D_{1,2,3}^*}{dt} = \partial_t + \frac{D_{1,2,3}^* x}{dt}\partial_x, \tag{120}$$

and where the characteristic equations are

$$\frac{D_1^* x}{dt} = u + c, \quad \frac{D_2^* x}{dt} = u - c, \quad \text{and} \quad \frac{D_3^* x}{dt} = u, \tag{121}$$

respectively.[15]

b.

Solve (117) - (119) numerically using the method of characteristics with fixed space increments Δx and time steps Δt. Disregard the wind- and bottom stress and look for solutions for $t > 0$ assuming that the initial condition at $t = 0$ is given by

$$h|_{t=0} = H + \Delta H \tanh(\kappa x), \quad u|_{t=0} = v|_{t=0} = 0 \tag{122}$$

The solution domain is $x \in \ < -\frac{1}{2}L, \frac{1}{2}L >$ where the two boundaries at $x = \pm\frac{1}{2}L$ are open boundaries. Furthermore we let $\kappa = 10/L$, $\Delta H = H/2$, $H = 100$ m and $L = 2000$ km. As open boundary condition we recommend to use the gradient condition or the "Flow Relaxation Scheme" (cf. the Lecture notes Chapter "Open boundary conditions").

[15] Hint: The problem is non-linear and hence the characteristics are not straight lines. Since we utilise fixed Δx and Δt they may from time to time cross the previous time level outside of the domain bounded by x_{j-1} on the left-hand side and x_{j+1} on the right-hand side. Remember to check whether this is the case before interpolating.

c.

Display the solution in graphical form by plotting the time evolution of h, u, v, as isolines in the x, t space (Hovmøller diagram).

12 Problem set: Upwelling in the Bay of Guinea

In their pioneering work *Adamec and O'Brien* (1978) showed how an observed coastal upwelling event in the Bay of Guinea that was not forced by the local wind could be explained by wind events in the western equatorial Atlantic, and hence by events removed far away from the bay itself. The observed upwelling was puzzling because it could not be explained by local wind forcing, which was the prevailing explanation of coastal upwelling phenomena at the time.

Their starting point was that the Russian research vessel R/V Passat, that was located on the Equator about 10^oW observed a significant and unexpected drop in the sea surface temperature (SST) *before* the seasonal upwelling in the Bay of Guinea was about to start. They also noted that the time difference between the two observations was just about right for an internal Kelvin wave to travel from the location of the research vessel to the Bay of Guinea[16]. They therefore hypothesized that the observed upwelling event in the Bay of Guinea was remotely forced by an equatorial trapped, upwelling Kelvin wave generated by a pressure disturbance in the western part of the equatorial Atlantic. Once created it would travel eastward across the Atlantic basin towards the African coast, where it transforms into two coastal internal Kelvin waves, one propagating northward and a second propagating southward. The northward propagating one would then after some time hit the Bay of Guinea causing an upwelling event as the wave passed by. To support their hypothesis *Adamec and O'Brien* (1978) performed an experiment using a fairly simple, linear and numerical ocean model.

The objective is to reproduce the solutions of *Adamec and O'Brien* (1978). What they did was to simulate the equatorial Kelvin wave using a linear, reduced gravity model. Thus the governing equations we will solve are,

$$\partial_t \mathbf{u} + \beta y \mathbf{k} \times \mathbf{u} + g' \nabla_H h = \frac{\boldsymbol{\tau}}{\rho H} + A \nabla_H^2 \mathbf{u}, \tag{123}$$

$$\partial_t h + H \nabla_H \cdot \mathbf{u} = 0, \tag{124}$$

where $\nabla_H = \mathbf{i}\partial_x + \mathbf{j}\partial_y$, $\beta = 10^{-11}$ is the change of the Earth's rotation with latitude (the β-plane approximation), $g' = \Delta\rho/\rho$ is the reduced gravity where $\Delta\rho = 2$kg/m^3.

The computational domain they used is an idealized rendition of the Atlantic basin as sketched in Figure 9. The basin is 5000 km long and stretches 1500 km to the north and south of the equator. The presence of the African continent is in the form of a rectangular box 2000 km long and 1000 km wide protruding into the basin from the northeast corner of the basin.

To solve (123) and (124) we use an Arakawa C-grid of mesh size $\Delta x = \Delta y = 25$km with the x-axis pointing eastward along the equator and the y-axis pointing northwards. Initially the ocean is at rest and in equilibrium with an upper layer equilibrium depth of $H = 50$m. The density difference between the upper and lower layer is $\Delta\rho = 2$kg/m^3. Use a time step of maximum 1/8 day. Furthermore let the eddy viscosity be $A = 10^2$m^2/s, and let the simulation span at least 120 days.

A motion is forced by applying a wind stress on the surface as displayed in Figure 10. The stress is pointing westward (from east towards west) so as to give upwelling at the equator.

[16]This is actually the same mechanism that is the basis for the explanation of the El Niño phenomenon in the Pacific Ocean (*Hurlburt et al.,* 1976). For details on El Niño confer the website http://www.coaps.fsu.edu/lib/Florida_Consortium/enso_links.shtml.

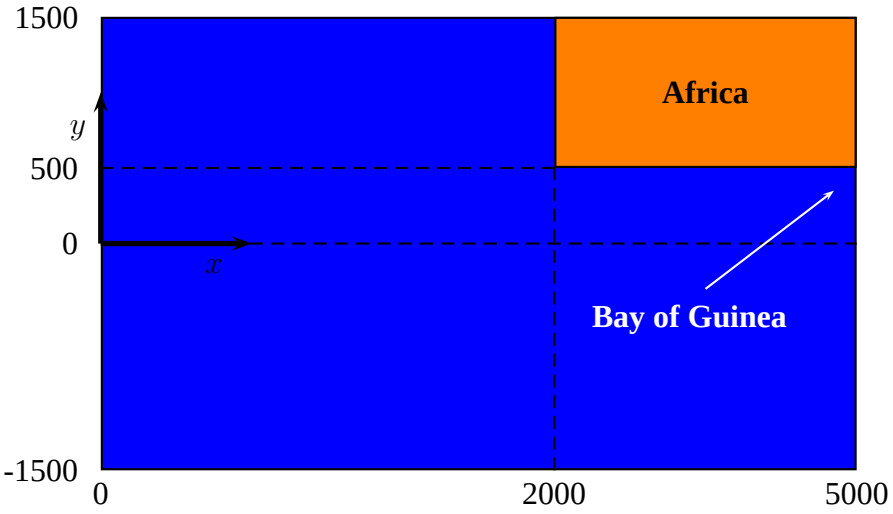

Figure 9: Sketch of the model domain for which (123) and (124) are to be solved. Numbers along axes are in kilometers.

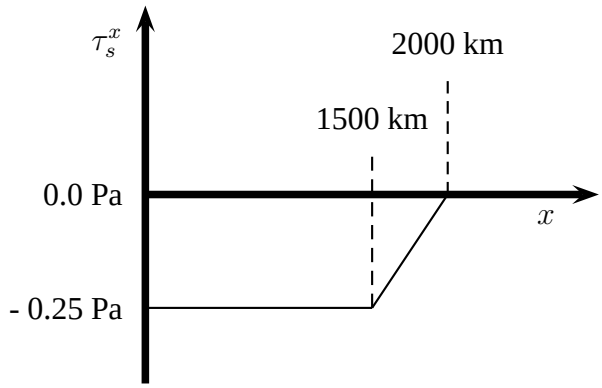

Figure 10: Displayed is the distribution of the zonal wind stress component in the zonal direction.

Furthermore it is limited to act in the western part of the basin only. Thus the wind stress is,

$$\tau_s^x = -\tau_0 \begin{cases} 1 & ; 0 < x \leq a \\ \frac{b-x}{b-a} & ; a < x \leq b \end{cases}, \quad \tau_s^y = 0. \tag{125}$$

where $\tau_0 = 0.025$ Pa, $a = 1500$ km and $b = 2000$ km. We observe that there is no wind stress acting in the north-south direction, and that it does not change with latitude, but depend on the longitude such that it is zero east of $x = 2000$ km.

In the finite difference approximation to (123) and (124) we use a CTCS[17] or leapfrog scheme. To avoid instabilities due to the diffusive term we employ the Dufort-Frankel scheme for these terms. The diffusion terms allows us to specify a no-slip condition at the walls. Thus at the

[17]CTCS - Centered in Time, Centered in Space.

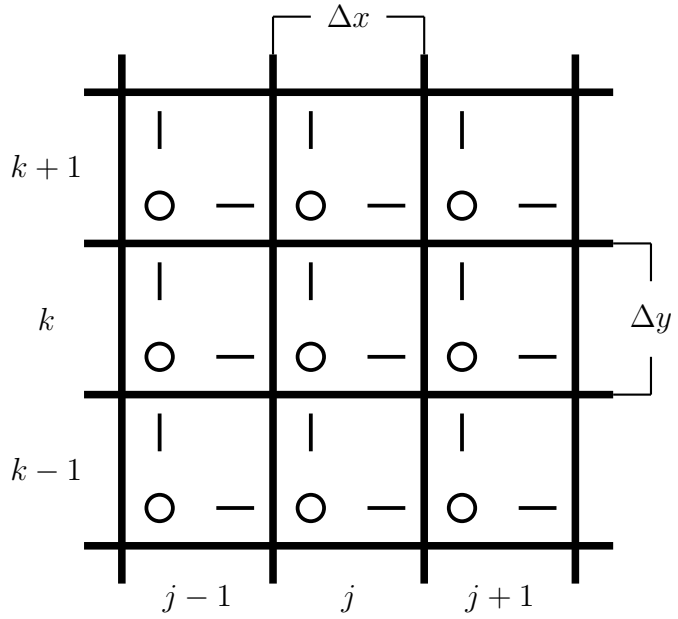

Figure 11: Displayed is the spatial grid and grid cells we use to solve (123) and (124) by numerical means. The grid increments are $\Delta x, \Delta y$, respectively in the x, y directions. There is a total of $J+1 \times K+1$ grid cells along the x- and y-axes, counted by using the dummy indices j, k. The coordinates of the grid points are $x_j = (j-1)\Delta x$ and $y_k = (k-1)\Delta y$, respectively. Circles, (O), correspond to h-points, horizontal dashes, $(-)$, to u-points, and vertical lines, $(|)$, to v-points.

solid walls both velocity components are zero. To make $v = 0$ along the eastern (and western) boundary we make use of so called mirror points outside of the boundary as sketched in Figure 12. By letting the value of v in the mirrored point equals the value of v just inside the boundary, the linearly interpolated value at the boundary itself becomes zero as required. A similar approach is used at the northern and southern boundaries to make u equal zero there. We notice that the physical (real) boundaries goes through the points where the normal to the boundary velocity component are located. Thus the eastern and western boundaries goes through u-points, while the northern and southern boundaries goes through v-points. With this configuration the coastlines fall exactly half way between the points where we compute the velocity component along the boundaries.

a.

Construct the finite difference approximation (FDA) to (123) and (124) using the required scheme as alluded to above and write it down.

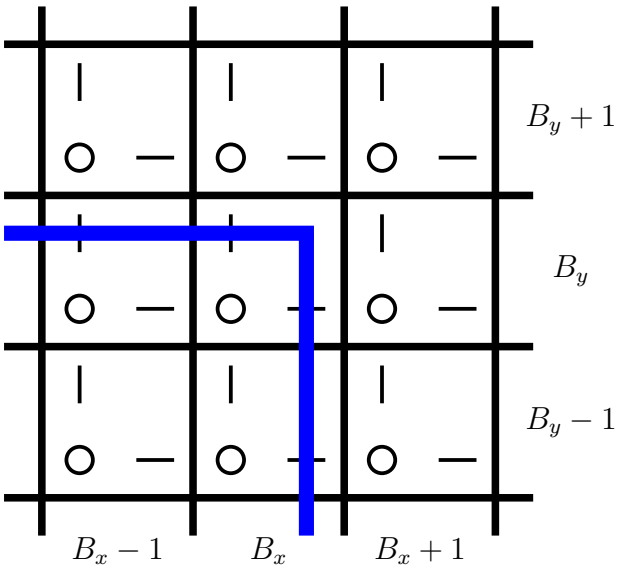

Figure 12: Displayed is the cells necessary to account for the no-slip boundary conditions at the walls. The walls are drawn as heavy solid blue lines. Here is displayed the right-hand corner located in the idealized Bay of Guinea (Figure 9). The three cells along the x-axis are numbered $B_x - 1$, B_x, $B_x + 1$, respectively, while along the y-axis the three cells are numbered $B_y - 1$, B_y, $B_y + 1$, respectively. The notation otherwise is as in Figure 11. Note that the five cells ($B_x + 1$,$B_y - 1$), ($B_x + 1$,B_y), ($B_x + 1$,$B_y + 1$), (B_x,$B_y + 1$) and ($B_x - 1$,$B_y + 1$) are outside of the land-sea boundary, that is on land. To account for the no-slip boundary condition of no velocity at the walls we mirror the along wall velocity component across the walls. Thus for the velocity points shown we let $v_{B_x+1B_y-1} = -v_{B_xB_y-1}$ and $u_{B_x-1B_y+1} = -u_{B_x-1B_y}$.

b.

Why is it permissible to use the diffusive, dissipative and inconsistent Dufort-Frankel scheme for the FDA of the diffusion terms? What are the advantages? Explain how you would construct a scheme that is forward in time and centered in space and still stable.

c.

Construct a graph displaying contour lines of the thickness deviation $\Delta h = H - h$ after 10, 50 and 100 days and with a contour interval of 5m. Furthermore, construct a similar graph showing the velocities of the upper layer at day 50.

d.

Next construct a graph showing the thickness deviation in a Hovmöller diagram. Let the vertical axis be the time axis ranging from 0 to 120 days, and let the horizontal axis be 6000 km long. Let the first part run along the equator from $x = 2500$ km to $x = 5000$ km, the next 500 km along the eastern boundary north of the equator, the next 2000 km along the southern coast of Africa, and the last 1000 km along the north-eastern boundary (west Africa).

e.

Use the Hovmöller diagram to estimate the phase speed of the Kelvin wave and compare it to the analytic one entering the governing equations. Discuss the result.

f.

Solve the non-linear version of (123) and (124), that is,

$$\partial_t \mathbf{u} + \mathbf{u} \cdot \nabla_H \mathbf{u} + \beta y \mathbf{k} \times \mathbf{u} + g' \nabla_H h = \frac{\boldsymbol{\tau}}{\rho H} + A \nabla_H^2 \mathbf{u}, \quad (126)$$

$$\partial_t h + \nabla_H \cdot (h\mathbf{u}) = 0, \quad (127)$$

and plot the results in a similar manner as for the linear case. Discuss differences and similarities.

h.

Finally, construct an animation (movie) displaying the linear as well as the nonlinear results.

References

Abramowitz, M., and I. Stegun (1965), *Handbook of Mathematical Functions - ninth printing*, Dover Publications, Inc.

Adamec, D., and J. J. O'Brien (1978), The seasonal upwelling in the Gulf of Guinea due to remote forcing, *J. Phys. Oceanogr.*, *8*, 1050–1060.

Blumen, W. (1972), Geostrophic adjustment, *Rev. Geophys. Space Phys.*, *10*, 485–528.

GESAMP (1991), (IMO/FAO/UNESCO/WMO/WHO/IAEA/UN/UNEP Joint Group of Experts on the Scientific Aspects of Marine Pollution), Coastal Modelling, *Tech. rep.*, International Atomic Energy Agency (IAEA), GESAMP Reports and Studies 43, 192 pp.

Gill, A. E. (1982), *Atmosphere-ocean dynamics*, *International Geophysical Ser.*, vol. 30, Academic Press.

Gjevik, B. (2009), *Flo og fjære langs kysten av Norge og Svalbard*, Farleia Forlag, Norway, ISBN 978-82-998031-0-6.

Gjevik, B., and L. P. Røed (1976), Storm surges along the western coast of Norway, *Tellus*, *28*, 166–182.

Hurlburt, H. E., J. C. Kindle, and J. J. O'Brien (1976), A numerical simulation of the onset of El Niño, *J. Phys. Oceanogr.*, *6*, 621–631.

LaCasce, J. H. (2009), Atmosphere-ocean dynamics, Class notes GEF4500, Dept. of Geosciences, University of Oslo, Norway.

Lynch, D. R., and A. M. Davies (1995), *Quantitative Skill Assessment for Coastal Ocean Models*, *Coastal and Estuarine Studies*, vol. 47, American Geophysical Union.

Martinsen, E. A., B. Gjevik, and L. P. Røed (1979), A numerical model for long barotropic waves and storm surges along the western coast of norway, *J. Phys. Oceanogr.*, *9*, 1126–1138.

Mesinger, F., and A. Arakawa (1976), Numerical methods used in atmospheric models, GARP Publication Series No. 17, 64 p., World Meteorological Organization, Geneva, Switzerland.

Røed, L. P. (1979), Storm surges in stratified seas, *Tellus*, *31*, 330–339.

Røed, L. P. (2011), Atmospheres and Ocean on Computers: Fundamentals, Lecture notes to GEF4510 fall 2011, Department of Geosciences, University of Oslo, P.O. Box 1022 Blindern, 0315 Oslo, Norway, 162 pp.

Røed, L. P. (2014), Atmospheres and Ocean on Computers: Fundamentals, Lecture notes to GEF4510 fall 2013, Department of Geosciences, University of Oslo, P.O. Box 1022 Blindern, 0315 Oslo, Norway, 220 pp.

Røed, L. P., and J. J. O'Brien (1983), A coupled ice-ocean model of upwelling in the marginal ice zone, *J. Geophys. Res.*, *29*(C5), 2863–2872.

Rossby, C. G. (1937), On the mutual adjustment of pressure and velocity distributions in certain simple current systems, *J. Mar. Res.*, *1*, 15–28.

Rossby, C. G. (1938), On the mutual adjustment of pressure and velocity distributions in certain simple current systems. part ii, *J. Mar. Res.*, *1*, 239–263.

Smolarkiewicz, P. K. (1983), A simple positive definite advection scheme with small implicit diffusion, *Mon. Wea. Rev.*, *111*, pp. 479.

Yoshida, K. (1959), A theory of the Cromwell current and of equatorial upwelling, *J. Oceanogr. Soc. Japan*, *15*, 154–170.